

Structure of ternary additive hard-sphere fluid mixtures

Alexander Malijevský* and Anatol Malijevský†
Institute of Chemical Technology, 16628 Prague 6, Czech Republic

Santos B. Yuste‡ and Andrés Santos§
Departamento de Física, Universidad de Extremadura, Badajoz, E-06071, Spain

Mariano López de Haro¶
Centro de Investigación en Energía, UNAM, Temixco, Morelos 62580, Mexico
(Dated: November 6, 2018)

Monte Carlo simulations on the structural properties of ternary fluid mixtures of additive hard spheres are reported. The results are compared with those obtained from a recent analytical approximation [S. B. Yuste, A. Santos, and M. López de Haro, *J. Chem. Phys.* **108**, 3683 (1998)] to the radial distribution functions of hard-sphere mixtures and with the results derived from the solution of the Ornstein–Zernike integral equation with both the Martynov–Sarkisov and the Percus–Yevick closures. Very good agreement between the results of the first two approaches and simulation is observed, with a noticeable improvement over the Percus–Yevick predictions especially near contact.

PACS numbers: 61.20.Ne, 61.20.Gy, 05.20.Jj, 82.60.Lf

I. INTRODUCTION

It is widely recognized that hard-sphere fluids have played a key role in the development and consolidation of liquid state theory. For these model systems, the link between structural properties and thermodynamics is immediate and simple, leading to rather straightforward expressions for the internal energy (which reduces to that of the ideal gas), and for the pressure equation, which only involves the contact values of the radial distribution functions (rdf) [1, 2, 3]. Nevertheless and despite the vast amount of literature devoted to their study, up to this day even the derivation of an explicit (exact) equation of state for these systems remains as an open problem. Under these circumstances, computer simulations have proved to be a useful way to derive structural and thermodynamic information as well as to allow the assessment of the many approximate theories proposed for them. These theories range from useful empirical expressions for the contact values of the rdf or the equation of state to the solution of Ornstein–Zernike (OZ) integral equations with a given closure. And of course both theory and simulation increase their complexity if one considers mixtures rather than single component fluids, so that it is not surprising that the available results are much scarcer for hard-sphere mixtures than for pure hard-sphere fluids. In fact, only binary mixtures have received some attention while results for ternary hard-sphere mixtures and those composed of more than three components are

particularly limited. As far as we are aware, there is only one computer simulation study on the structure and thermodynamics of the hard-sphere additive ternary mixture [4], where diameter ratios $1:2:\frac{10}{3}$ were considered at three densities and two compositions. One should also mention that Schaink [5] has performed a simulation study of a *non-additive* hard-sphere ternary mixture where the diameter ratios 1:1:1 were taken; the same mixture was studied by Gazzillo [6] from an integral equation approach. On the theoretical side, it is imperative to mention the pioneering work of Lebowitz [7, 8], who solved the Percus–Yevick equation for a multicomponent mixture of additive hard spheres. Also important are the papers by Boublík [9], Grundke and Henderson [10], and Lee and Levesque [11], in which they introduced the contact values, now referred to as the Boublík–Grundke–Henderson–Lee–Levesque (BGHLL) contact values, leading to the Boublík–Mansoori–Carnahan–Starling–Leland (BMCSL) equation of state [9, 12]. Apart from these, in the case of multicomponent mixtures to our knowledge there is only some work by Gazzillo [13] on the thermodynamic criteria of local stability, a paper by Boublík [14] on rdf, the scaled field particle theory of isotropic hard particle fluids of Rosenfeld [15] and the studies carried out by some of us [16, 17]. In these latter studies an interesting behavior of the rdf $g_{ij}(r)$ was predicted, but it could not be assessed in view of the then absence of available computer simulation data to compare with.

On another vein, it is clear that ternary mixtures are typical in nature and technology. For instance, air is essentially a mixture of nitrogen, oxygen, and argon (the concentration of other components is much lower), and sea water is a mixture of H_2O , Na^+ and Cl^- . There is also a number of industrially important chemical reactions among three components, *e.g.* the synthesis of

*Alexandr.Malijevsky@vscht.cz

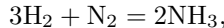
†Anatol.Malijevsky@vscht.cz

‡santos@unex.es

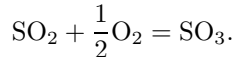
§andres@unex.es

¶malopez@servidor.unam.mx

ammonia



or in ecology, *e.g.*



Ternary mixtures of molecules whose interaction includes an attractive part have been studied from perturbation theory and van der Waals one-fluid theory [18, 19, 20].

In view of the above, the aim of this paper is to provide simulation results for hard-sphere additive ternary mixtures that will serve as a starting point to assess the accuracy and validity of some theoretical approaches. Specifically, we will examine five ternary systems at the same packing fraction and with fixed diameter ratios, so that they are only different because of their composition. Two of these cases correspond to mixtures in which the biggest spheres occupy over 50% of the available volume, followed in volume occupation by the intermediate sized spheres and finally by the smallest spheres. A third system is considered in which all species share equitatively the available volume, while in the last two systems it is the intermediate spheres which occupy the smallest volume and either the biggest or the smallest sized ones follow in volume occupation. The theoretical approaches that we will consider will be the solution of the Ornstein–Zernike equation with both the Percus–Yevick [7] and the Martynov–Sarkisov [21] closures and the (approximate) expressions for the rdf of a hard-sphere mixture derived in Ref. [16].

The paper is organized as follows. In order to make the paper self-contained, in Sect. II we recall the main results of the theoretical approaches to derive the structural properties of hard-sphere mixtures. Section III provides some details of the simulation and the comparison between simulation data and the different theoretical approximations. We close the paper in Sect. IV with a discussion and some concluding remarks.

II. THEORETICAL APPROXIMATIONS TO THE STRUCTURAL PROPERTIES OF MULTICOMPONENT MIXTURES OF ADDITIVE HARD SPHERES

An n -component mixture made of ρ_i hard spheres (of diameter σ_i) per volume unit may be characterized by $2n - 1$ parameters (for instance, the $n - 1$ mole fractions $x_i = \rho_i/\rho$, the $n - 1$ size ratios σ_i/σ_1 and the packing fraction $\eta \equiv \sum_{i=1}^n \eta_i$, $\eta_i = \frac{\pi}{6}\rho_i\sigma_i^3$ denoting the partial packing fraction corresponding to species i) and involves $n(n + 1)/2$ rdf $g_{ij}(r)$. Within the usual integral equation approach, the OZ equation is a set of $n(n + 1)/2$ coupled equations

$$\gamma_{ij}(r) = \rho \sum_{k=1}^n x_k \int d\mathbf{r}' h_{ik}(|\mathbf{r}'|) c_{kj}(|\mathbf{r} - \mathbf{r}'|), \quad (1)$$

where $h_{ij}(r) \equiv g_{ij}(r) - 1$ and c_{ij} denote the total and the direct correlation functions, respectively, and $\gamma_{ij} = h_{ij} - c_{ij}$ is the series function. A general closure for the OZ equation may be written in the form

$$c_{ij}(r) = \exp[-\beta u_{ij}(r) + \gamma_{ij}(r) + B_{ij}(r)] - 1 - \gamma_{ij}(r), \quad (2)$$

where $u_{ij}(r)$ is the interaction potential and B_{ij} is the bridge function. In this work we consider two approximations to the bridge function: the classical Percus–Yevick (PY) theory

$$B_{ij}(r) = \ln[1 + \gamma_{ij}(r)] - \gamma_{ij}(r), \quad (3)$$

and the Martynov–Sarkisov (MS) [21] theory

$$B_{ij}(r) = \sqrt{1 + 2\gamma_{ij}(r)} - 1 - \gamma_{ij}(r). \quad (4)$$

We solved the OZ equation with these closures in the case of ternary mixtures ($n = 3$) using an algorithm that is a direct extension of the method proposed for one-component simple fluids [22]. In our numerical implementation in this paper, we used $N = 2048$ grid points with a step size $\Delta r = 0.01$. In the case of the PY closure, the rdf can also be obtained by numerical inversion of analytical expressions in Laplace space [16]. Both methods give undistinguishable results, what gives confidence on the accuracy of the numerical solution of the MS closure.

An alternative method to obtain an approximate expression for $g_{ij}(r)$ for a multicomponent mixture was introduced in Ref. [16]. We will refer to this method as the RFA approach since it stemmed out of a generalization of a rational function approximation to structural quantities in a simple hard-sphere fluid [23]. Working in the Laplace space and defining $G_{ij}(s) = \int_0^\infty dr e^{-sr} r g_{ij}(r)$, the foregoing approach implies that G_{ij} is assumed to adopt the following functional form [16, 24]:

$$G_{ij}(s) = \frac{e^{-s\sigma_{ij}}}{2\pi s^2} \sum_{k=1}^n L_{ik}(s) [(1 + \alpha s)I - A(s)]^{-1}_{kj}, \quad (5)$$

where

$$L_{ij}(s) = L_{ij}^{(0)} + L_{ij}^{(1)} s + L_{ij}^{(2)} s^2, \quad (6)$$

$$A_{ij}(s) = \rho_i \sum_{p=0}^2 \varphi_p(s\sigma_i) \sigma_i^{p+1} L_{ij}^{(2-p)}, \quad (7)$$

with

$$\varphi_p(x) \equiv x^{-(p+1)} \left[\sum_{m=0}^p \frac{(-x)^m}{m!} - e^{-x} \right]. \quad (8)$$

There are two basic requirements that $G_{ij}(s)$ must satisfy. First, since $g_{ij}(r) = 0$ for $r < \sigma_{ij}$, with $\sigma_{ij} = (\sigma_i + \sigma_j)/2$, and the contact values $g_{ij}(\sigma_{ij}^+) = \text{finite}$,

this implies that (i) $\lim_{s \rightarrow \infty} s e^{s\sigma_{ij}} G_{ij}(s) = \text{finite}$. Second, the isothermal compressibility $\kappa_T = \text{finite}$, so that (ii) $\lim_{s \rightarrow 0} [G_{ij}(s) - s^{-2}] = \text{finite}$. Condition (i) is verified by construction. On the other hand, condition (ii) yields two *linear* sets of n^2 equations each, whose solution is straightforward:

$$L_{ij}^{(0)} = \lambda + \lambda' \sigma_j + 2\lambda' \alpha - \lambda \sum_{k=1}^n \rho_k \sigma_k L_{kj}^{(2)}, \quad (9)$$

$$L_{ij}^{(1)} = \lambda \sigma_{ij} + \frac{\lambda'}{2} \sigma_i \sigma_j + (\lambda + \lambda' \sigma_i) \alpha - \frac{\lambda}{2} \sigma_i \sum_{k=1}^n \rho_k \sigma_k L_{kj}^{(2)}, \quad (10)$$

where $\lambda \equiv 2\pi/(1-\eta)$ and $\lambda' \equiv (\lambda/2)^2 \rho \langle \sigma^2 \rangle$ with $\langle \sigma^p \rangle \equiv \sum_{i=1}^n x_i \sigma_i^p$. The parameters $L_{ij}^{(2)}$ and α are arbitrary, so that conditions (i) and (ii) are satisfied regardless of their choice. In particular, if one chooses $L_{ij}^{(2)} = \alpha = 0$, the approximation given by Eq. (5) coincides with the PY solution. If, on the other hand, we fix given values for $g_{ij}(\sigma_{ij}^+)$, we get the relationship $L_{ij}^{(2)} = 2\pi \alpha \sigma_{ij} g_{ij}(\sigma_{ij}^+)$; thus, only α remains to be determined. Finally, if we fix κ_T , we obtain an algebraic equation for α of degree $2n$.

In previous work with the RFA approach [16, 24] the BGHLL values of $g_{ij}(\sigma_{ij}^+)$ and κ_T given by the BMCSL equation of state [9, 12] were considered. In this work, however, we will use a different approximation which was recently proposed by three of us [25]. Following this proposal, we assume that

$$g_{ij}(\sigma_{ij}^+) = F(\eta, z_{ij}), \quad (11)$$

where $z_{ij} \equiv (\sigma_i \sigma_j / \sigma_{ij}) \langle \sigma^2 \rangle / \langle \sigma^3 \rangle$, and take the function $F(\eta, z)$ to be *universal* in the sense that it is a common function for all the pairs ij . Further F is forced to comply with known exact relations in the point particle, equal size and colloidal limits. Under these circumstances, the simplest functional form that F may adopt is a quadratic function of z :

$$F(\eta, z) = F_0(\eta) + F_1(\eta)z + F_2(\eta)z^2, \quad (12)$$

where the coefficients are explicitly given by

$$F_0(\eta) = \frac{1}{1-\eta}, \quad (13)$$

$$F_1(\eta) = 2(1-\eta)g(\sigma^+) - \frac{2-\eta/2}{1-\eta}, \quad (14)$$

$$F_2(\eta) = \frac{1-\eta/2}{1-\eta} - (1-2\eta)g(\sigma^+). \quad (15)$$

Here, $g(\sigma^+)$ denotes the contact value of the radial distribution function of a simple hard-sphere fluid. For this

latter, we take the one corresponding to the Carnahan-Starling equation of state [26], namely $g_{CS}(\sigma^+) = (1-\eta/2)/(1-\eta)^3$. With such choice, Eqs. (11) and (12) become

$$g_{ij}(\sigma_{ij}^+) = \frac{1}{1-\eta} + \frac{3}{2} \frac{\eta(1-\eta/3)}{(1-\eta)^2} z_{ij} + \frac{\eta^2(1-\eta/2)}{(1-\eta)^3} z_{ij}^2, \quad (16)$$

and the compressibility factor for the mixture, from which κ_T may be readily derived, reads

$$Z(\eta) = Z_{\text{BMCSL}}(\eta) - \frac{\eta^3}{(1-\eta)^2} \frac{\langle \sigma^2 \rangle}{\langle \sigma^3 \rangle^2} (\langle \sigma \rangle \langle \sigma^3 \rangle - \langle \sigma^2 \rangle^2), \quad (17)$$

where the compressibility factor associated with the BMCSL equation of state [9, 12] is given in the present notation by

$$Z_{\text{BMCSL}}(\eta) = \frac{1}{1-\eta} + \frac{3\eta \langle \sigma \rangle \langle \sigma^2 \rangle}{(1-\eta)^2 \langle \sigma^3 \rangle} + \frac{\eta^2(3-\eta) \langle \sigma^2 \rangle^3}{(1-\eta)^3 \langle \sigma^3 \rangle^2}. \quad (18)$$

Equation (16) represents in general a significant improvement over the BGHLL contact values [25]. On the other hand, the BMCSL equation of state (18) performs slightly better than Eq. (17). Although the RFA can be implemented by making any choice for $g_{ij}(\sigma_{ij}^+)$ and κ_T , here we have taken, in addition to the contact values (16), the isothermal compressibility associated with Eq. (17) in order to enforce thermodynamic consistency.

III. SIMULATION DETAILS AND RESULTS

We used the standard NVT-Monte Carlo method with periodic boundary conditions, employing a cell index algorithm with six different cell sizes corresponding to a number of interactions. The simulation cubic box contained $N = 2700$ particles in each case but one (case C), where $N = 6777$ particles were used.

The initial system with no overlaps was generated by random insertion of particles to an originally empty box. The sequence we used is the following: the largest particles were inserted first and the smallest ones at the end. Particles were mixed during this procedure. Starting with this initial configuration, we generated the Monte Carlo chain as follows. The acceptance ratio of trial moves was adjusted to 10–15% for all the components. Each run was divided into 21 blocks, each of which included about 10^9 of the equilibrium configurations generated and contained 300–500 analyses of the calculation of the rdf $g_{ij}(r)$ in the whole range of 1200 intervals $r_i \pm \Delta r/2$ (where the step size was $\Delta r = 5 \times 10^{-3} \sigma_1$) up to a distance $6\sigma_1$. The analysis was performed after 1000 trial moves per particle (more precisely after 1000N trial moves of a randomly chosen particle). The first block was then discarded and the next 20 were used to sample the configuration space, calculate mean values for the entire run and estimate the errors.

The systems we examined had the same packing fraction $\eta = 0.49$ and fixed diameter ratios $\sigma_2/\sigma_1 = 2$ and $\sigma_3/\sigma_1 = 3$ (for convenience and without loss of generality we have chosen the value of the diameter of the smallest spheres to be always 1) so that their only difference lies in the composition. They are identified as

- (A) $x_1 = 0.7, x_2 = 0.2, x_3 = 0.1,$
 $\eta_1/\eta = 0.14, \eta_2/\eta = 0.32, \eta_3/\eta = 0.54,$
- (B) $x_1 = 0.6, x_2 = 0.2, x_3 = 0.2,$
 $\eta_1/\eta \simeq 0.08, \eta_2/\eta \simeq 0.21, \eta_3/\eta \simeq 0.71,$
- (C) $x_1 = \frac{216}{251}, x_2 = \frac{27}{251}, x_3 = \frac{8}{251},$
 $\eta_1/\eta = \eta_2/\eta = \eta_3/\eta = \frac{1}{3},$
- (D) $x_1 = 0.85, x_2 = 0.05, x_3 = 0.10,$
 $\eta_1/\eta \simeq 0.22, \eta_2/\eta \simeq 0.10, \eta_3/\eta \simeq 0.68,$
- (E) $x_1 = 0.90, x_2 = 0.07, x_3 = 0.03,$
 $\eta_1/\eta \simeq 0.396, \eta_2/\eta \simeq 0.247, \eta_3/\eta \simeq 0.357.$

These systems have been located in two different ternary diagrams, one with respect to mole fractions and the other one corresponding to partial packing fractions, shown in Figs. 1 and 2, respectively. In these diagrams we have also included the two systems with diameter ratios $\sigma_2/\sigma_1 = 2$ and $\sigma_3/\sigma_1 = 10/3$ that were studied by Šindelka and Boublík [4] and which we have labeled SB1 ($x_1 = x_2 = x_3 = \frac{1}{3}; \eta_1/\eta \simeq 0.022, \eta_2/\eta \simeq 0.174, \eta_3/\eta \simeq 0.804$) and SB2 ($x_1 = \frac{1}{2}, x_2 = \frac{1}{3}, x_3 = \frac{1}{6}; \eta_1/\eta \simeq 0.054, \eta_2/\eta \simeq 0.285, \eta_3/\eta \simeq 0.661$). It should be pointed out that cases A and B (as well as the systems SB1 and SB2) correspond to the situation $\eta_1 < \eta_2 < \eta_3$, while in case D one has $\eta_2 < \eta_1 < \eta_3$, in case E $\eta_2 < \eta_3 < \eta_1$ and in case C $\eta_1 = \eta_2 = \eta_3$. This, in our view, allows us to examine the very different situations that arise depending on which species occupies the largest volume.

The results of our calculations, both theoretical and from the simulations, are displayed in Figs. 3–8. In Fig. 3 we show the contact values for all five systems as functions of the parameter z_{ij} defined below Eq. (11). In this instance we have considered the PY, BGHLL, MS, and scaled particle theory (SPT) values [15, 27], as well as those given by Eq. (16). In the case of the MS approximation we actually get a set of points that have been joined by a line interrupted at $z_{33} = 1.481$ (case D) since there is no convergence in cases C and E. The fact that this line is a smooth one shows that the numerical values obtained from the MS approximation seem to be consistent with the “universality” assumption (11). The comparison with the simulation data indicates that for $z > 1$ the new proposal, Eq. (16), improves over the BGHLL prescription (while for $z < 1$ it is only slightly worse) and both are clearly superior to the SPT recipe. The PY values are very poor, while the MS approximation tends to underestimate the contact values for $z > 1$. This provides some support to the use of Eq. (16) and

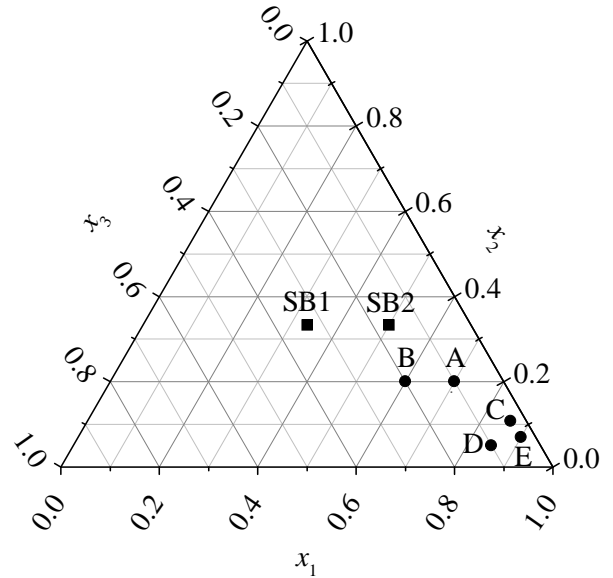


FIG. 1: Ternary diagram showing the mole fractions of the five cases A–E considered in this paper, as well as the two cases (SB1 and SB2) considered by Šindelka and Boublík [4].

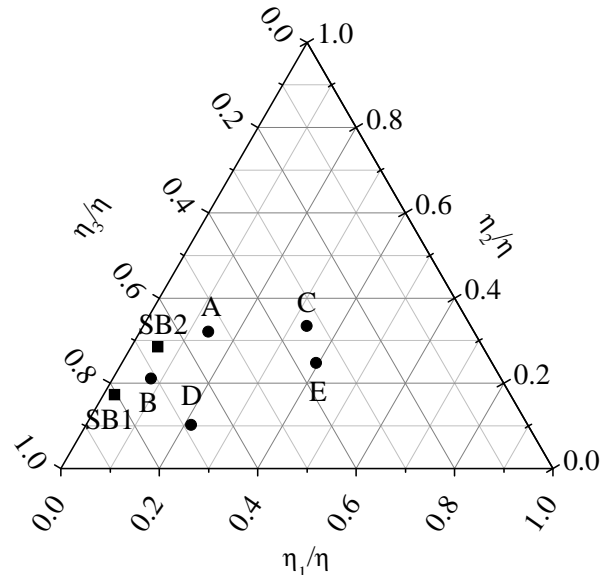


FIG. 2: Ternary diagram showing the (relative) packing fractions of the five cases A–E considered in this paper, as well as the two cases (SB1 and SB2) considered by Šindelka and Boublík [4].

Eq. (17) (this latter to compute κ_T) within the approximate scheme to derive the rdf $g_{ij}(r)$ for ternary mixtures that was introduced in Ref. [16] and briefly sketched in the previous section.

Figures 4–8 show all the rdf $g_{ij}(r)$ ($i, j = 1, 2, 3$) as functions of the shifted distances $r - \sigma_{ij}$ for the five different systems considered. Also included in these figures are insets with an enlarged scale around $g_{ij}(r) = 1$ in which

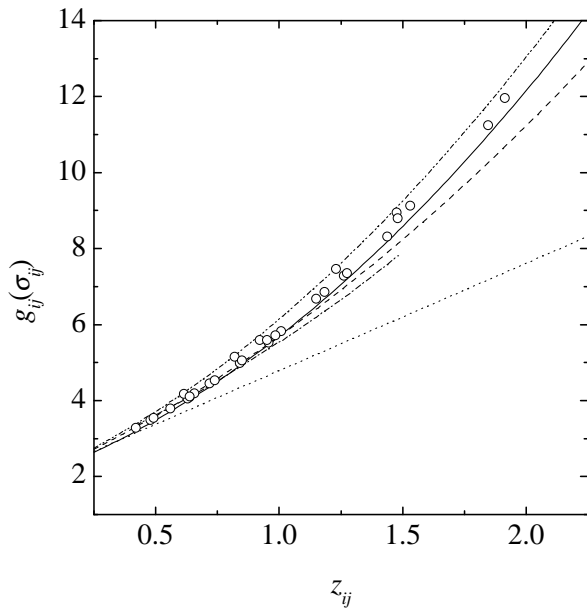


FIG. 3: Plot of the contact value $g_{ij}(\sigma_{ij}^+)$ as a function of the parameter $z_{ij} = (\sigma_i \sigma_j) \langle \sigma^2 \rangle / \langle \sigma^3 \rangle$ for ternary additive hard-sphere mixtures at a packing fraction $\eta = 0.49$. The circles are simulation data for the five cases A–E considered in this paper. The lines are theoretical predictions: Eq. (16) (—), BGHLL (---), SPT (- · -), MS (- · ·), and PY (···).

we have plotted $g_{ij}(r)$ versus the actual rather than the shifted distance. It should be noted that, as said before, the solution to the OZ equation with the MS closure did not converge for cases C and E. This is a consequence of the fact that a term under the square root in Eq. (4) becomes negative at high densities; the authors of the MS closure speculate that the lack of convergence may be a signal of phase transition [28]. The analysis of this conjecture is beyond the scope of this paper. The study of Figs. 4–8 indicates the following. The RFA approach provides an excellent overall agreement with the simulation results, which is especially good in the region around contact. Something similar occurs with the solution to the OZ equation with the MS closure, except that this solution tends to underestimate the contact value of g_{23} and g_{33} . The PY closure clearly yields the poorest results especially in the region around contact. All three theoretical approaches lead to almost identical results beyond the first minimum and exhibit a rich fine structure as was already pointed out for another ternary system in Ref. [16]. The fact that the simulation results also exhibit this structure is in our view remarkable. It should be noted that there are slight quantitative differences around the first minimum, which is more pronounced in the theoretical solutions than in the simulation. Except for cases C and E where the fine structure is rather similar, in the other three cases the fine structure is case dependent. As may be observed in Fig. 2, cases C and E correspond to

a situation where all partial packing fractions are rather similar. Interestingly enough, when this happens, *i.e.* no species is dominant with respect to volume occupation, all the rdf $g_{ij}(r)$ relax to 1 following an ordered sequence of damped oscillations. Finally, it is also worth mentioning that, for a given system, the form of the fine structure of the $g_{ij}(r)$ is *almost* the same for all pairs. In fact, such fine structure seems to evolve smoothly as σ_{ij} increases ($\sigma_{11} = 1, \sigma_{12} = 1.5, \sigma_{22} = \sigma_{13} = 2, \sigma_{23} = 2.5, \sigma_{33} = 3$) as one can easily see by following the sequence top panel left, top panel right, middle panel right, middle panel left, bottom panel right, bottom panel left in Figs. 4, 5, and 7.

IV. CONCLUDING REMARKS

The results of the previous section deserve some further comments. As far as the simulations are concerned, we have here provided further data on the thermodynamic and structural properties of ternary additive hard-sphere fluid mixtures that extend and complement those of Ref. [4]. The quality and reliability of these new data is reflected in their ability to capture the rich fine structure that had been observed earlier in connection with the RFA approach [16]. Both the RFA results and the ones derived from the solution of the OZ equation with the MS closure are in very good agreement with the simulation data, but the latter give less accurate contact values, the OZ equation needs to be solved numerically, and it presents convergence problems when the partial packing fractions of all three species have similar values. In any case these two theoretical approaches do represent an improvement over the Percus–Yevick theory. Finally, we have only carried out a preliminary qualitative analysis of the rich fine structure that arose in the systems we examined. By restricting ourselves to a fixed total packing fraction and given diameter ratios, we attempted to investigate the effect of partial volume occupation by each species on the resulting structure. It thus appears interesting to assess the effect of different total packing fractions and (or) size ratios. We may address these and other related issues in multicomponent systems in the future.

Acknowledgments

The two first authors (A. M. and A. M.) acknowledge support by the Center for Complex Molecular Systems and Biomolecules (Project LN00A032 of the Ministry of Education, Youth and Sports of the Czech Republic). A.S. and S.B.Y. acknowledge partial support from the Ministerio de Ciencia y Tecnología (Spain) through grant No. BFM2001-0718. We thank Prof. Labík for helpful discussions.

-
- [1] D. A. McQuarrie, *Statistical Mechanics* (Harper & Row, New York, 1976).
- [2] T. Boublík, I. Nezbeda, and K. Hlavatý, K., *Statistical Thermodynamics of Simple Liquids and Their Mixtures* (Elsevier, Amsterdam, 1980).
- [3] J. S. Rowlinson and F. J. Swinton, *Liquids and Liquid Mixtures*, 3rd ed. (Butterworth, London, 1982)
- [4] M. Šindelka, and T. Boublík, *Fluid Phase Equilibria* **143**, 13 (1998).
- [5] H. M. Schaink, *Physica A* **210**, 113 (1994).
- [6] D. Gazzillo, *Mol. Phys.* **84**, 303 (1995).
- [7] J. L. Lebowitz, *Phys. Rev.* **133**, 895 (1964).
- [8] E. Paschinger, A. Reiner, and G. Kahl, *Mol. Phys.* **94**, 743 (1998).
- [9] T. Boublík, *J. Chem. Phys.* **53**, 471 (1970).
- [10] E. W. Grundke, and D. Henderson, *Mol. Phys.* **24**, 2619 (1972).
- [11] L. L. Lee and D. Levesque, *Mol. Phys.* **26**, 1351 (1973).
- [12] G. A. Mansoori, N. F. Carnahan, K. E. Starling, and T. W. Leland, *J. Chem. Phys.* **54**, 1523 (1971).
- [13] D. Gazzillo, *Mol. Phys.* **83** 1171 (1994).
- [14] T. Boublík, *Mol. Phys.* **91**, 161 (1997).
- [15] Y. Rosenfeld, *J. Chem. Phys.* **89**, 4272 (1998).
- [16] S. B. Yuste, A. Santos, and M. López de Haro, *J. Chem. Phys.* **108**, 3683 (1998).
- [17] S. B. Yuste, A. Santos, and M. López de Haro, *An. Fís.–Monogr.* **4**, 169 (1998).
- [18] K. Fotouh and K. Shukla, *Chem. Eng. Sci.* **51**, 4923 (1996); 4933 (1996).
- [19] M. Bluma and U. K. Deiters, *Phys. Chem. Chem. Phys.* **1**, 4307 (1999).
- [20] Y. S. Wei and R. J. Sadus, *Phys. Chem. Chem. Phys.* **1**, 4329 (1999).
- [21] G. A. Martynov and G. N. Sarkisov, *Mol. Phys.* **49**, 1495 (1983).
- [22] S. Labík, A. Malijevský, and P. Voňka, *Mol. Phys.* **56**, 709 (1985).
- [23] S. B. Yuste and A. Santos, *Phys. Rev. A* **43**, 5418 (1991).
- [24] S. B. Yuste, A. Santos and M. López de Haro, *Mol. Phys.* **98**, 439 (2000).
- [25] A. Santos, S. B. Yuste, and M. López de Haro, *J. Chem. Phys.* **117**, 5785 (2002).
- [26] N. F. Carnahan and K. E. Starling, *J. Chem. Phys.* **51**, 635 (1969).
- [27] J. L. Lebowitz, E. Helfand, and E. Praestgaard, *J. Chem. Phys.* **43**, 774 (1965).
- [28] G. A. Martynov, private communication.

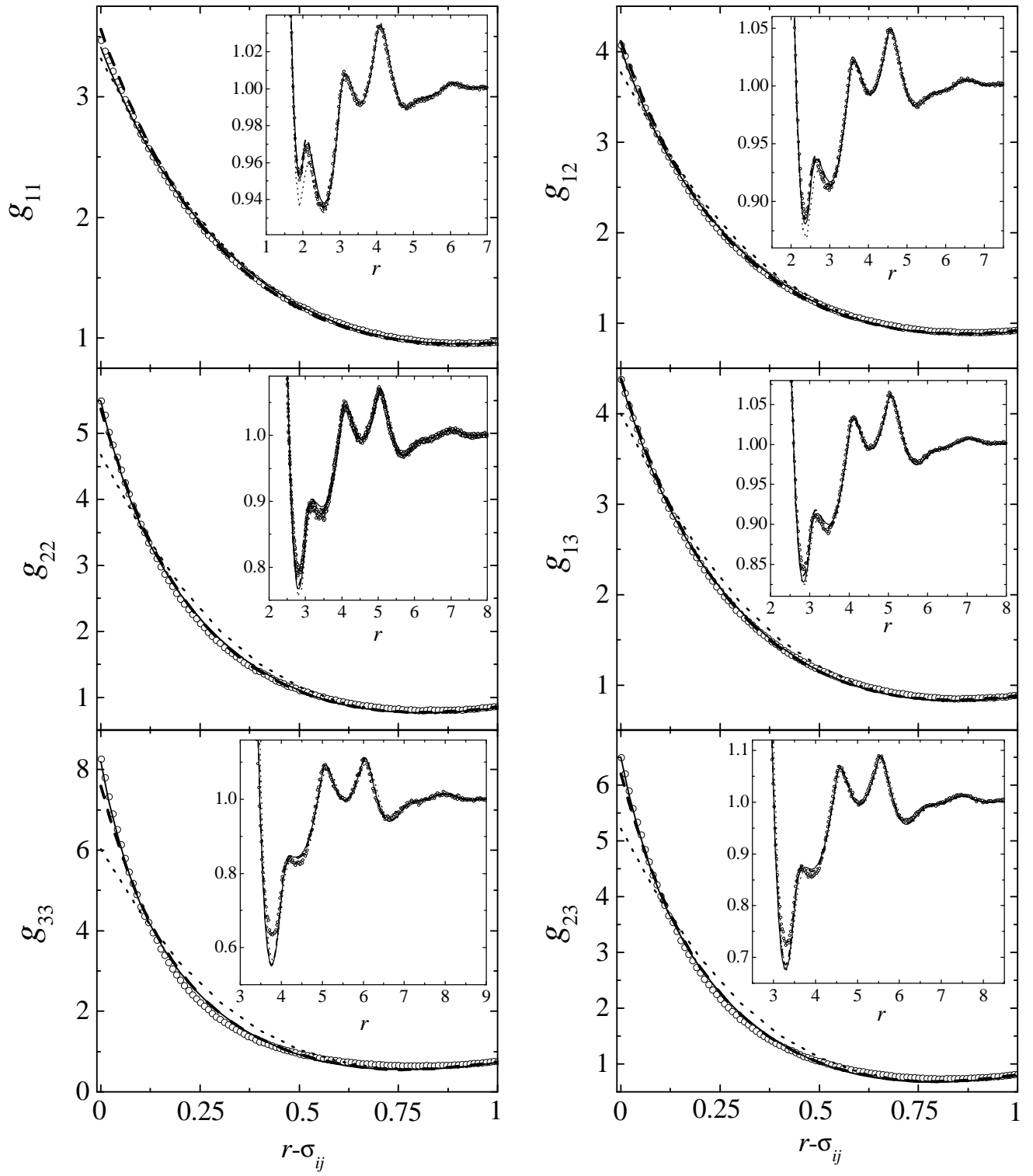


FIG. 4: Radial distribution functions $g_{ij}(r)$ for a ternary mixture with diameters $\sigma_1 = 1$, $\sigma_2 = 2$, $\sigma_3 = 3$ at a packing fraction $\eta = 0.49$ in case A ($x_1 = 0.7$, $x_2 = 0.2$, $x_3 = 0.1$). The circles are simulation results, the solid lines are the RFA predictions, the dotted lines are the PY predictions, and the dashed lines are the MS predictions.

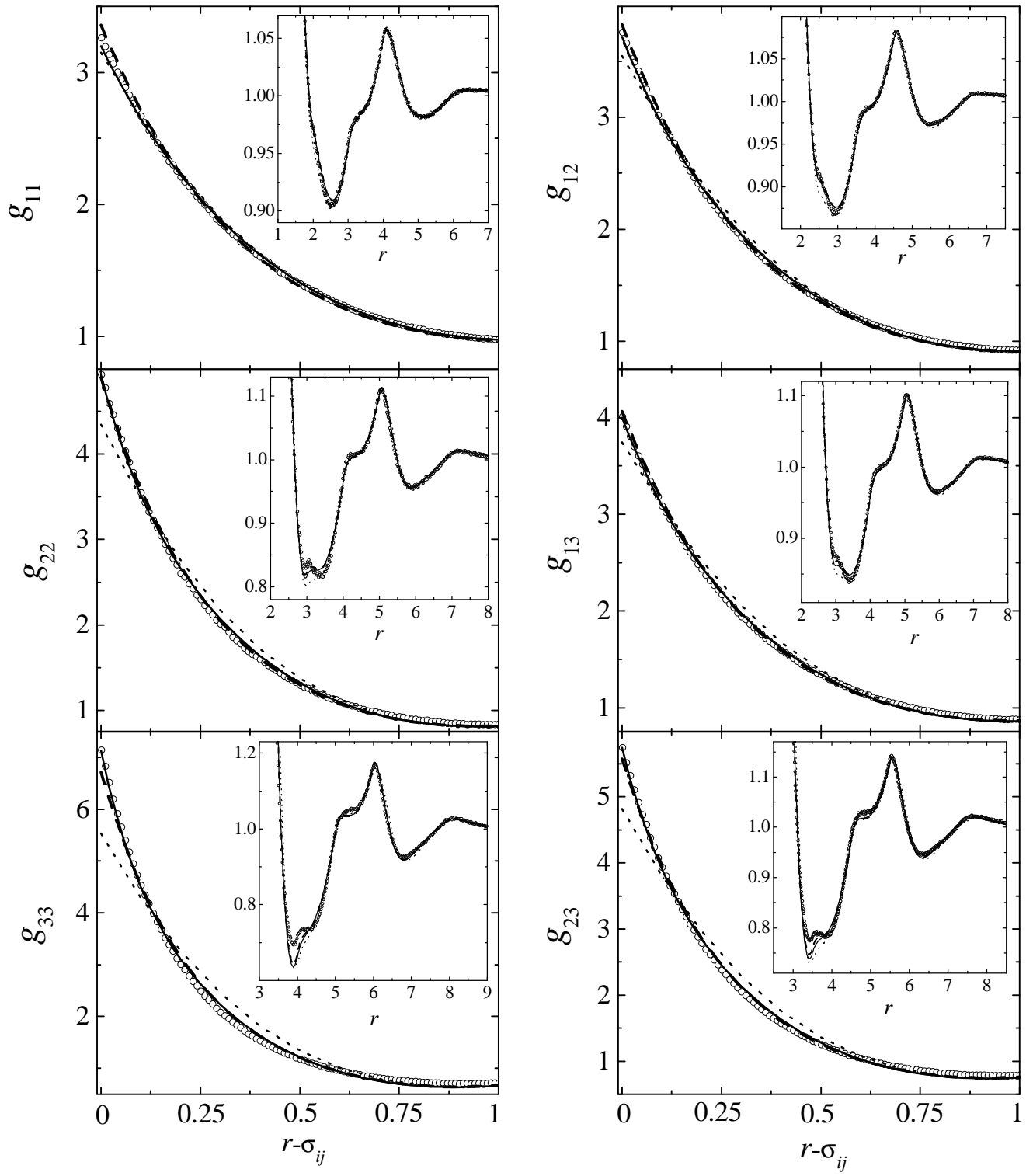


FIG. 5: The same as in Fig. 4, but in case B ($x_1 = 0.6$, $x_2 = 0.2$, $x_3 = 0.2$).

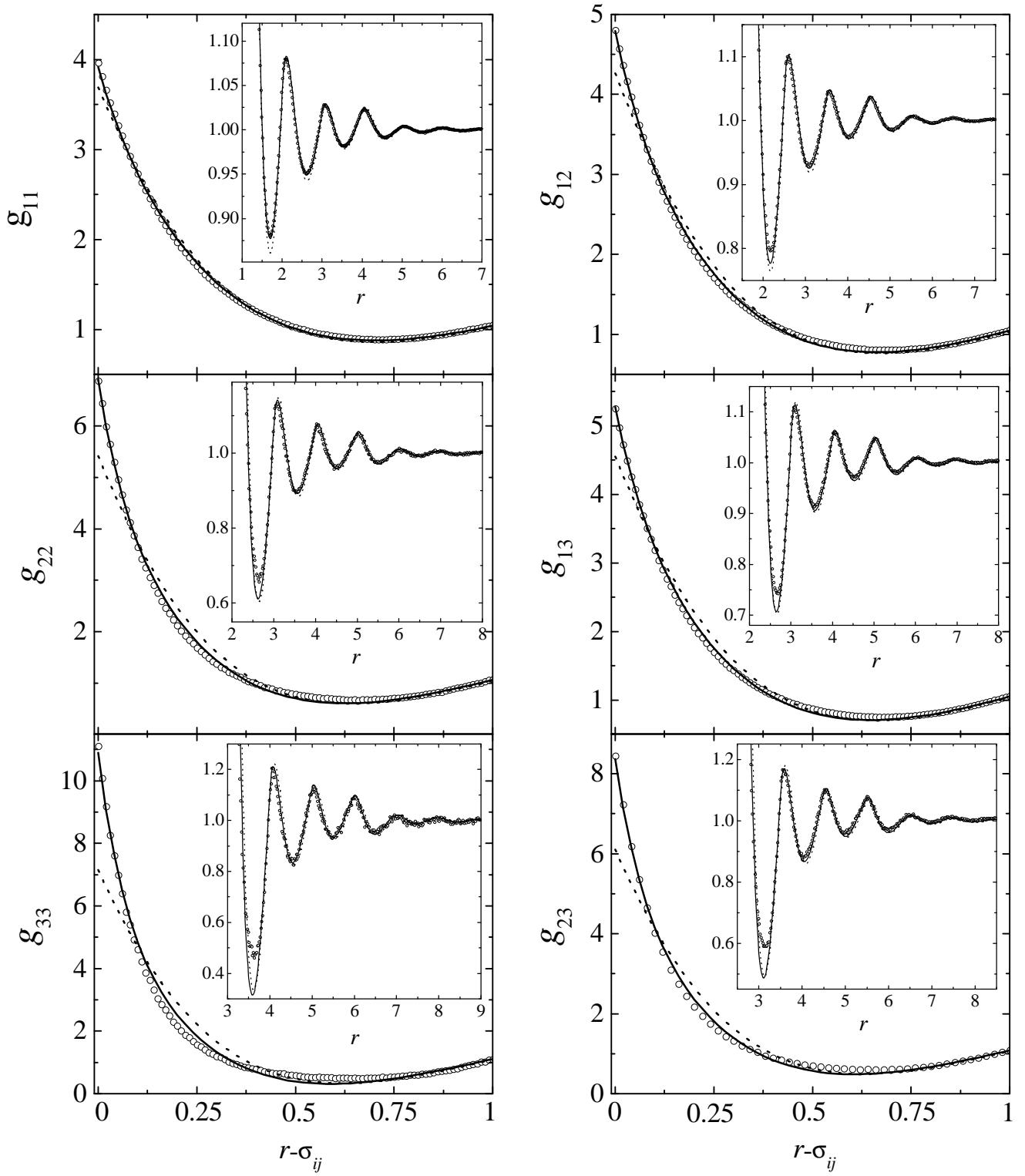


FIG. 6: The same as in Fig. 4, but in case C ($x_1 = \frac{216}{251}$, $x_2 = \frac{27}{251}$, $x_3 = \frac{8}{251}$). Note that the OZ equation with the MS closure fails to converge in this case.

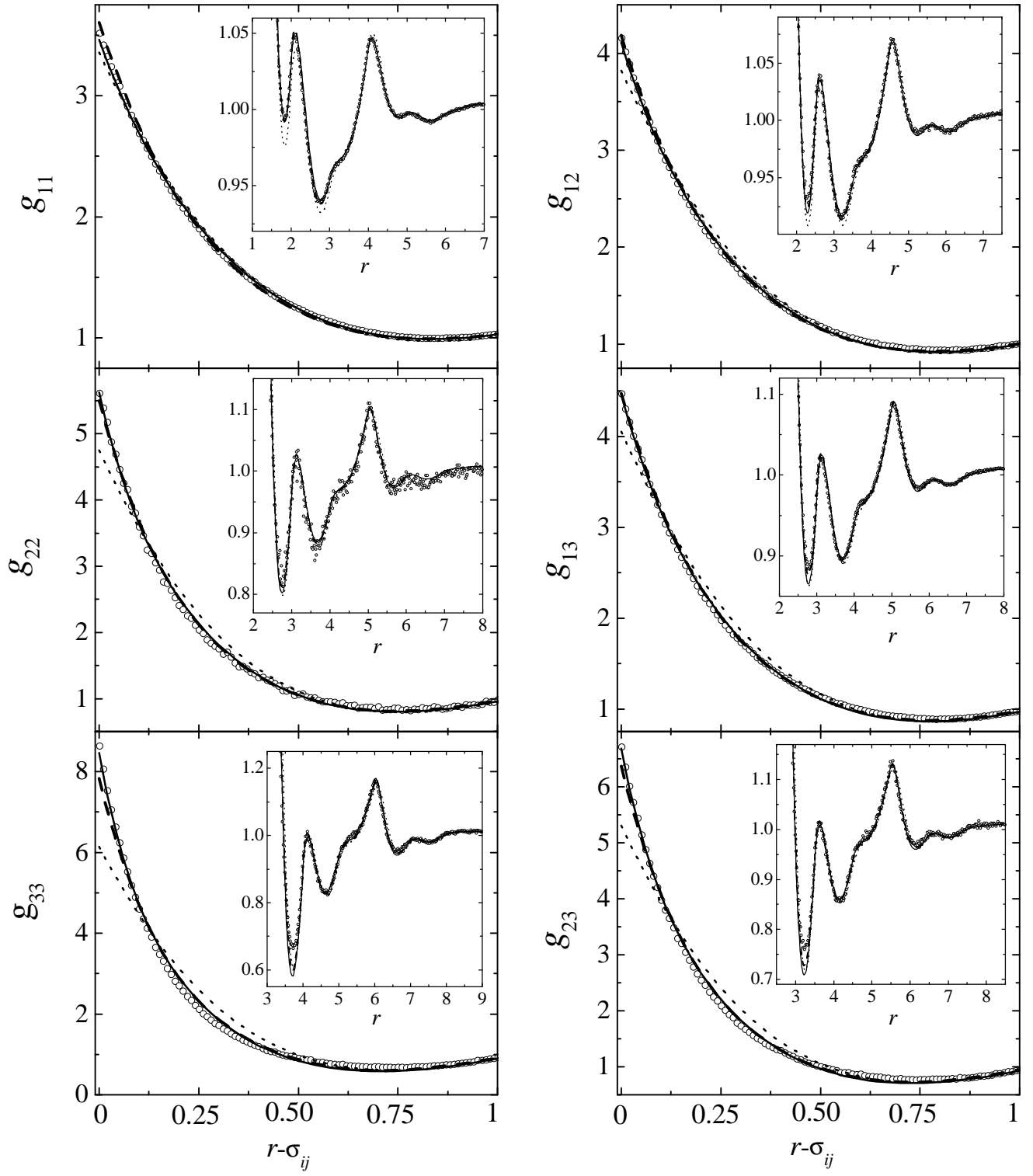


FIG. 7: The same as in Fig. 4, but in case D ($x_1 = 0.85$, $x_2 = 0.05$, $x_3 = 0.10$).

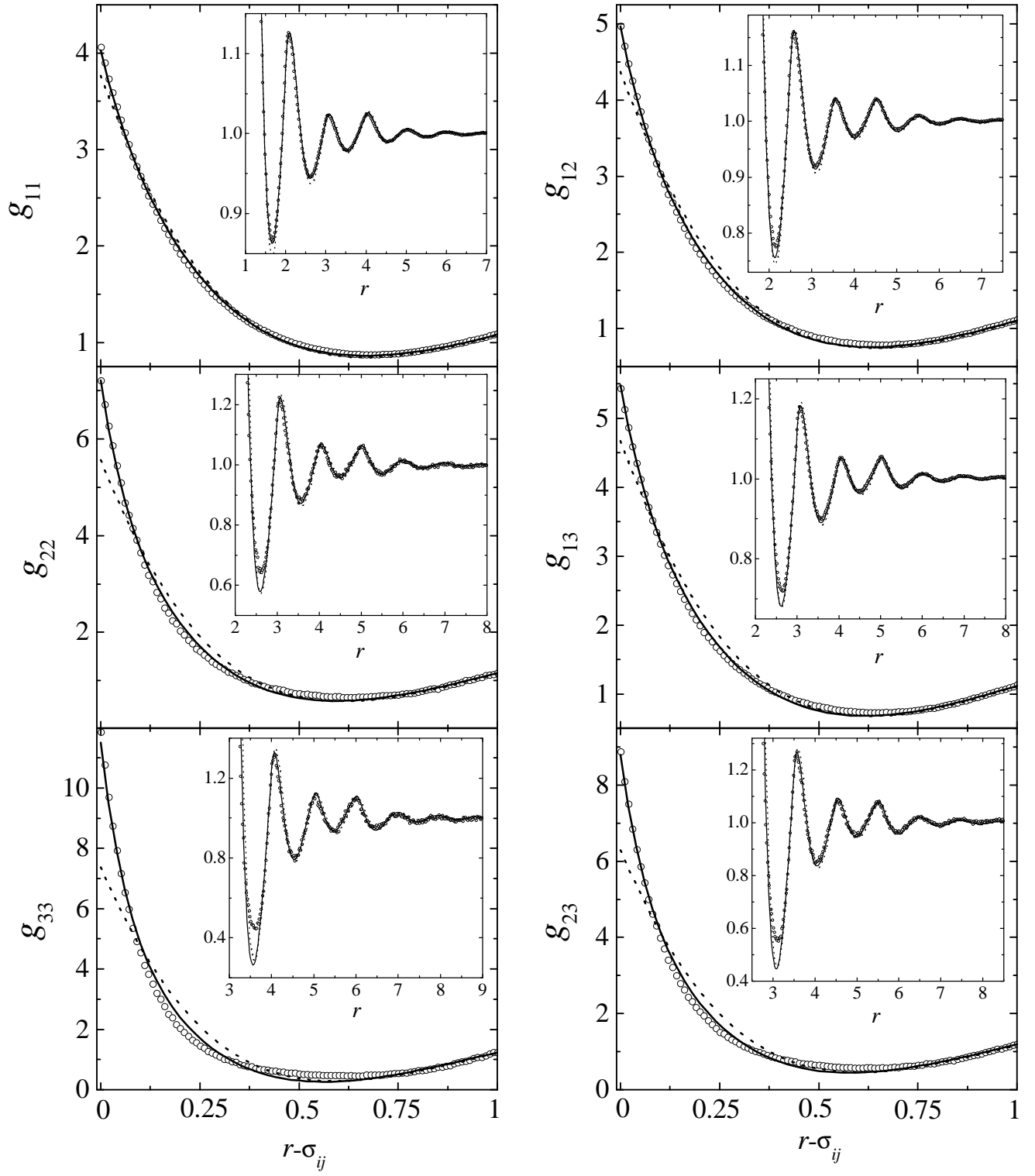


FIG. 8: The same as in Fig. 4, but in case E ($x_1 = 0.90$, $x_2 = 0.07$, $x_3 = 0.03$). Note that the OZ equation with the MS closure fails to converge in this case.